19th Australasian Fluid Mechanics Conference
Melbourne, Australia
8-11 December 2014

In-Situ Detection of Nanoparticles in Turbulent Flames Using Laser Induced Emissions

D. Bartos[1], M. Dunn[1], A. Masri[1], A. D'Anna[2], M. Sirignano[2]

[1] School of Aerospace, Mechanical and Mechatronic Engineering,
The University of Sydney, Sydney Australia
[2] Dipartimento di Ingegneria Chimica, Universita``'Federico II"di Napoli,
Piazzale V. Tecchio, 80, 80125 Napoli, Italy

Abstract

This paper extends the application of laser induced emission techniques employed to measure soot nano-particles to turbulent flames. Such methodologies were developed to measure the evolution of soot in laminar flames with detection of nano-particles in the range 1-10nm (Mode I), as well as larger soot aggregates, in the range 10-100nm (Mode II). The new laser based system has been specifically designed to account for the short transients of turbulent flows. It employs a 30ps laser pulse at 266nm and 6mJ/pulse. Four fast photomultiplier tubes located at the exit plane of a spectrometer are used to detect elastic scattering at 266nm, UV and visible laser induced fluorescence centred at 300nm and 450nm, and laser induced incandescence at wavelengths larger than 550nm. Preliminary measurements in laminar ethylene flames are examined and compared to previous in-situ and ex-situ measurement to verify the reliability of the experimental apparatus. Validity of the technique in a turbulent flame has been explored. Estimates of the spatial resolution and limits of applicability in terms of minimum particle number and detection limits in highly sooting flames due to excessive laser induced incandescence levels are examined.

Introduction

This research is part of a larger project aimed at enhancing current knowledge of the evolution of soot particles in turbulent flames. Extensive research has already been undertaken on sooting laminar premixed and diffusion flames and excellent reviews on this topic are available [1-3]. Measurements of soot evolution in laminar flames [4-14] reveal the existence of a bimodal number density distribution with small nanoparticles (referred to as Mode I) in the size range less than 10nm and larger particles (referred to as Mode II) up to hundreds of nanometers which are generally individuated as mature soot. Mode I particles are formed and directly linked with the nucleation of polycyclic aromatic hydrocarbons (PAHs) which are generally well correlated with mixture fraction. The exact processes involved in the nucleation of these particles remain the subject of intense research. Mode II particles that are not a function of mixture fraction, have a well-known chain-like structure in which primary particles can be distinguished within aggregates.

Detailed measurements in turbulent sooting flame are scarce, less advanced than in laminar ones, and largely limited to mean quantities of soot volume fraction. Early work was largely based on soot scattering and extinction methods [15-17] and seminal work of Kent and Honnery [16] in turbulent diffusion flames of ethylene has established that soot volume fraction does not correlated with mixture fraction. Laser induced incandescence (LII) then became more prevalent extending measurement of soot volume fraction to turbulent piloted [18] as well as bluff-body [19] stabilised flames of ethylene. More advanced techniques such NTLAF to measure temperature in sooting flames [6], joint LII and velocity field [20] as well as LIF of PAH species [21] are emerging providing extremely relevant information about soot formation in turbulent flames. Computations of soot structure of turbulent flames are probably more advanced than the available data and have been largely based on RANS-CMC approach, calculation of Kronenburg et al. [22] providing a typical example. More recently, LES started to take precedence using the method of moments along a various models of soot evolution. The link between the gaseous and soot fields is obtained either via presumed pdf methods [19, 23, 24], linear eddy models [25, 26] or by solving joint transport equations for the joint pdf [27].

The objective of this paper is to communicate a new experimental technique for the in-situ measurement of Mode 1 and Mode 2 soot particles in turbulent flames. The technique is inspired by the wide range of methods that have been developed and applied to laminar flames for the measurement and soot and its precursors. Short laser excitation at 266nm and with a pulse duration of 30ps, is applied to induce emissions. These are monitored at a range of wavelengths including elastic scattering, fluorescence bands between 300 and 450nm as well as the LII band at wavelength larger than 550nm. A key element of this new setup is the ability to monitor the temporal evolution of the collected signals. This paper will limit its scope to a description of the system and a validation in laminar flames. Preliminary measurements in turbulent diffusion flames of ethylene are made and samples are shown here only to demonstrate that the technique is capable of measuring, both the soot volume fraction and mean size of Mode 1 and Mode 2 soot. To the knowledge of the authors, this is the first time such measurements are made in a turbulent flame, albeit at modest Reynolds numbers. A detailed analysis of the data collected will appear in a subsequent paper.

Experimental setup

Burners and flames

Two types of flame were investigated: first a laminar flame was studied to check consistency with previous measurements and then a turbulent flame. In laminar flows the signal can be averaged over many frames resulting in a high signal to noise (S/N) ratio. This, however, cannot be applied in turbulent flames so improved detection methods are necessary to yield single-shot signals with sufficiently high S/N. For the laminar flames, a Santoro style burner with an inner diameter, d=12.5 mm and co-flow diameter, D=70 mm is used. The non-premixed flame was run at atmospheric conditions with ethylene (0.23 SLPM) as fuel in a co-flow of air (10 SLPM) which was adjusted slightly to

keep the flame stable. The visible laminar flame length was 70 mm but the very tip was flickering slightly causing measurements at 70 mm to contain some intermittency.

The second case is a modestly turbulent jet flame with Reynolds number, Re=4800. Although the turbulence level is modest, this flame provides an adequate test for the approach since it still features a significant level of intermittency. The burner is piloted with a fuel jet diameter d=4 mm surrounded by a pilot annulus (D=18mm) which is recessed by 15 mm upstream of the jet exit plane. The pilot is a premixed hydrogen, acetylene and air and the main fuel jet is a mixture of ethylene and nitrogen (1/1 by volume). This diluted fuel mixture was chosen to produce sufficient soot without having the LIF signals corrupted by natural incandescence or LII. Table 1 lists the flow rates employed in the various streams. The visible flame length is about 450mm.

Flame:	**Flow Rate (SLPM)**
Ethylene	5
Nitrogen	5
Pilot:	**Flow Rate (SLPM)**
Hydrogen	0.7
Acetylene	0.7
Air	14

Table 1. Turbulent flame flowrates.

Optical Set-up

The collection setup consists of two distinct sections that operate in parallel. The flame is excited by the 4th Harmonic (266nm) of a mode locked Nd:YAG laser (Ekspla PL2251 Series Laser) at 10 Hz, pulse length of 30 ps and 6 mJ/pulse. The short pulse length ensures that the temporal response of the LIF signals is not distorted. The 266 nm wavelength laser pulse is suitable for LIF excitation of PAH while still causing LII in larger soot particles [4, 13, 28]. Additionally, this wavelength will reduce fragmentation and C_2 emissions that would interfere with the LIF and LII signals. Florescence from this incident wavelength can be attributed to two broadband emissions of particles; a UV band and a visible band peaking around 320 nm and 420 nm respectively. These two spectra indicate the presence of precursor PAH, Mode I nanoparticles with the UV-LIF and visible LIF being indicative of PAH aggregates of sizes about 2 to 4nm and 5 to 10nm respectively. The probe volume of the focused laser is estimated at a diameter of 15 microns. The entire setup is schematized in Fig. 1.

The first section of collection consists of the Oriel Spectrometer coupled with an intensifier and ICCD camera. This collection system is designed to attain spectrally resolved information of the excited probe volume. This system is critical in identifying the key spectral bins of interest being laser scattering, LIF and LII. However, this setup is limited temporally as it has a relatively long exposure of 1 ms, and thus the signal is integrated over this time. The key spectral bins are identified in Fig. 2. The strongest signal is the scattering of 266nm and some residual 532nm allowing easy spectral calibration. A theoretical response of this system was calculated such that relative comparisons can be made between signals.

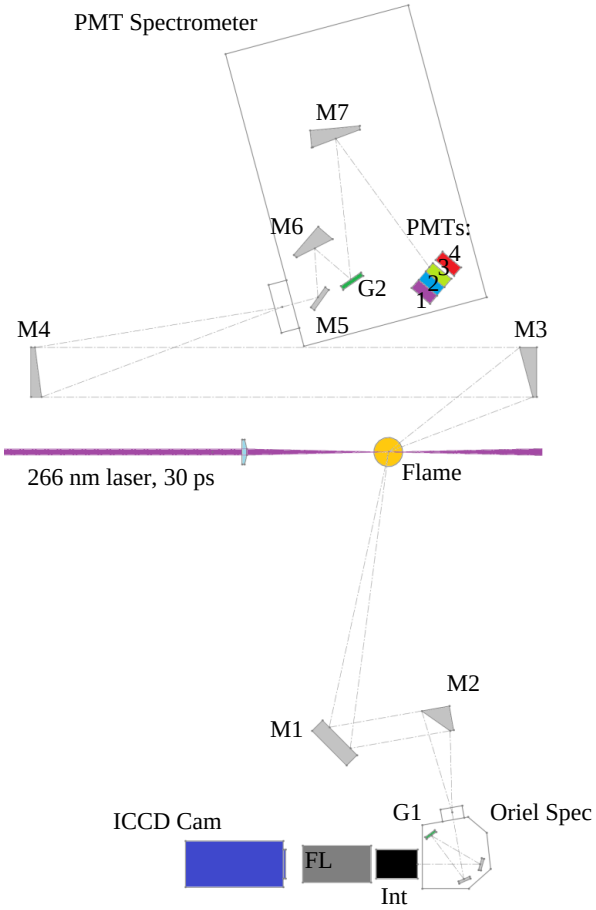

Figure 1. Experimental setup.

Equipment:	**Description:**
M1	Spherical Aluminium Mirror: d =75 mm, fl = 500 mm
M2	90 Degree Off-Axis Parabolic Aluminium Mirror: d = 50.8 mm pfl = 95.3 mm
M3,M7	30 Degree Off-Axis Parabolic Aluminium Mirror: d = 101.6 mm pfl = 304.8 mm
M4	15 Degree Off-Axis Parabolic Aluminium Mirror: d = 101.6 mm pfl = 508 mm
M5	Flat UV Enhanced Mirror: d = 50mm
M6	45 Degree Off-Axis Parabolic Aluminium Mirror: d = 76.2 mm pfl = 152.4 mm
G1	Ruled Diffraction Grating: 300 lines/mm, 300nm Blaze Wavelength
G2	Ruled Diffraction Grating: 600 lines/mm, 300 nm Blaze Wavelength
Oriel Spec	Oriel Spectrometer: 125mm, MODEL 77400, 200 μm slit width
Int	Intensifier: d = 18mm,
FL	Focusing lenses
ICCD Cam	ICCD Camera: La Vision Flowmaster 3
PMT 1,2,3	Photomultiplier tube: Hamamatsu H10721-210
PMT 4	Photomultiplier tube: Hamamatsu H10721-20
fl = focal length d = diameter pfl = parent focal length of parabolic mirror	

Table 2. Equipment.

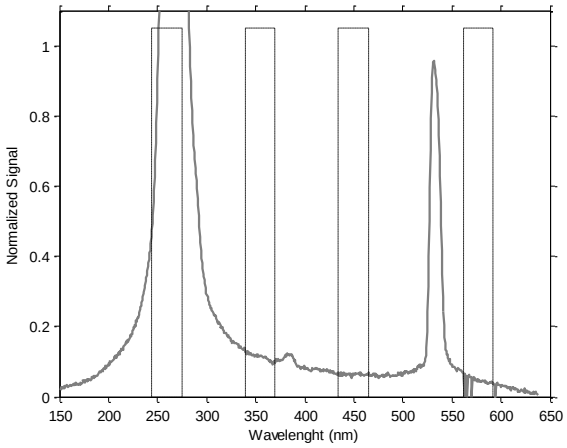

Figure 2. Example spectrum captured by setup. Note scattering peaks at 266 nm and 532 nm. PMT bins indicated by dotted sections.

The second collection path is designed to acquire temporally resolved data of select spectral bins. Four Photomultiplier tubes (PMT) are mounted at the focal plane of a custom built spectrometer modified in order to achieve a desirable spectral distribution that was large enough to fit PMTs within distinct spectral bins. The four PMTs are placed to intecept one of the following signals: 266 scattering, UV LIF, Visible LIF, LII. See Table 3 for the spectral bins collected by the PMTs. The PMTs are connected to a high speed oscilloscope (Tektronix DSA70404C), allowing for detailed temporal analsis of the signals. This setup has a very low signal to noise ratio, but is dependant on the gain set to the PMTs. Different gains are set to each PMT as signal strenghts differ between PMTs. As seen in Fig. 2 the 266 nm scattering is by far the strongest signal, in fact too strong that it would saturate PMT1 even at the lowest practical gain. To avoid this issue and also to reduce excess signal splash onto the adjacent PMTs a high pass filter (WG 305) was placed in front of the slit of the PMT Spectrometer. Some subtraction of the scattering signal is still required from the LIF and LII signals. The collection of the temporal evolution of the LIF and LII signals is crucial in understanding the structure of emitting particles. The LIF emission lifetime is expected to be significantly diffident depending if the PAH aggregates are cross-linked structures or stacked.

PMT	Wavelength bin (nm)	Gain (volts)
1	244 to 275	0.75
2	339 to 370	0.75
3	434 to 465	0.75
4	562 to 592	0.85 laminar, 0.97 turbulent

Table 3. PMT wavelenght bins.

Both sides of the collection system utilize focusing mirrors to collect the light. Although mirros provide aditional challenges in alignment, they were neccesary to avid spectral aberation that is inherent in lenses. Due the broad wavelenght band that is analysed with this technique, spectral aberation would have a large influence on signal collection.

Data Processing

A relativley short laser pulse was used to avoid distortion of the decaying LIF and LII traces. However the rise time of the PMTs is approximatley 1 ns (dependant on gain). This convolutes the LIF and LII signals as shown in Eq. 1. The aquired signal I_T is convoluted by of the incident signal I_L, which is the laser puse as seen by the PMT and the exponential fluorecence decay I_E. Signal I_T is expected to be a gaussian with rise time close to 1 ns. This is in agreement witht the scattering signal seen in Fig. 3 displaying a rise time of t=0.84 ns. A deconvolution of the LIF and LII signals is necessary to obtain the real decay signal I_E.

$$I_T = I_L * I_E \tag{1}$$

$$I_E(t) = e^{(-\frac{1}{\tau}t)} \tag{2}$$

The decay time τ is found by curve fitting I_E with the approxiation of a single exponetial decay as in Eq. 2. The fitted convoluted curve (example seen in Fig. 3) closely matches the LIF signal up to around 14ns while giving a decay time of 7ns. This is consitent with what is expected from aggregate and gasphase PAHs with low numbers of rings [13, 29]. Some literature suggests that fluorescence decay consists of multi-eponential decay and would allow better match to the signal [29]. This need sto be further investigated.

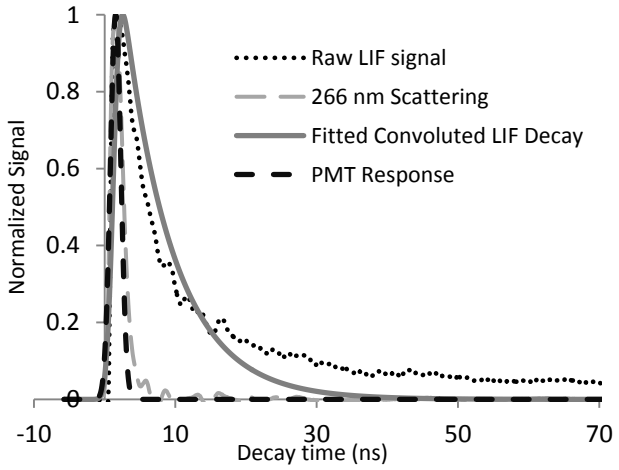

Figure 3. Example signal response and convolution.

Results

Centreline measurements were collected along the length of the laminar flame to visulize the progession of soot. At each measurement location, an average of 150 shots is taken and the results from the four measured signals are shown in Fig. 4 height above burner (HAB). Peaks for scattering at 266nm, LIF-UV, LIF-visible as well as LII occur at HAB=30-40mm. The peak in LIF-UV, LIF-visible ocurs closer to HAB=30mm indicating that soot inception of Mode I particles is occurring within this region and this is consistent with earlier results [13, 29]. It should be noted that elastic scattering from fuel and other gases would also contribute to the high signal detected at 266nm. Measurements at 60 and 70 mm were affected by the intermitency of the flame. Results presented in Fig. 4 confirm that the approach re-produces the results expected from laminar sooting flames.

Figure 5 shows centreline profiles of all four signals (scattering at 266nm, LIF-UV, LIF-visible as well as LII) measured at different HAB in the turbulent flame. The first observation to make is that the signal level is significantly lower than that seen in the laminar flame. The intermittency of the turbulent flame results in an order of magnitude drop in average

signal, highlighting the importance of obtaining high signal to noise ratio. The scattering signal increases with downstream distance and this is expected since the visibly incandescing region of the flame which contains higher levels of soot particles is approached. The high level of LIF-UV and LII at HAB=50 and 100 mm is believed to be interference due to other fluorescing species and possible fragmentation of the ethylene. With this consideration, both LIF-UV and visible signals increase and peaks around HAB=300 mm in the zone prior to the visibly sooting region. A similar trend is also noted for LII. These preliminary results are encouraging since they are consistent with the qualitative features of the turbulent flames. Further improvements in the signal quality are being pursued to enable processing of the instantaneous signals as required for the turbulent flames.

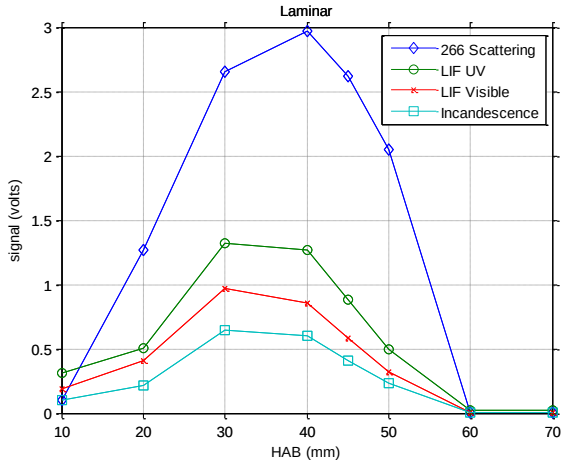

Figure 4. PMT signals collected at various HAB along the centreline of laminar ethylene flame.

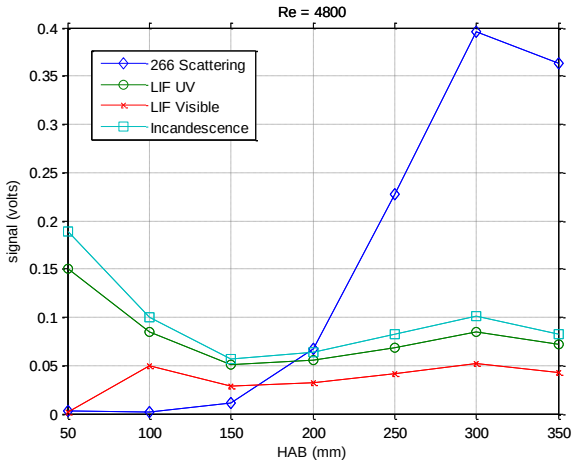

Figure 5. Preliminary, mean PMT signals collected along the centreline of a urbulent diluted ethylene flame.

Conclusion

Using laser excitation at 266nm with a pulse duration of 30ps, emissions from laminar and turbulent flames of ethylene are excited and monitored at a range of wavelengths including elastic scattering, fluorescence bands between 300 and 450nm as well as the LII band at wavelength larger than 550nm. The measurements in laminar flames are consistent with the literature. While more refinements are needed, preliminary results indicate that this technique is applicable in turbulent flames as well.

Acknowledgements

This research is supported by the Australian Research Council.

References

[1] A. D'Anna, Proceedings of the Combustion Institute **32 (**2009) 593-613.
[2] P. Desgroux, X. Mercier, and K.A. Thomson, Proceedings of the Combustion Institute **34 (**2013) 1713-1738.
[3] H. Wang, Proceedings of the Combustion Institute **33 (**2011) 41-67.
[4] S. Bejaoui, X. Mercier, P. Desgroux, and E. Therssen, Combustion and Flame.
[5] H. Bladh, N.-E. Olofsson, T. Mouton, J. Simonsson, X. Mercier, A. Faccinetto, P.-E. Bengtsson, and P. Desgroux, Proceedings of the Combustion Institute.
[6] Q.N. Chan, P.R. Medwell, P.A.M. Kalt, Z.T. Alwahabi, B.B. Dally, and G.J. Nathan, Proceedings of the Combustion Institute **33 (**2011) 791-798.
[7] M. Commodo, G. Tessitore, G. De Falco, A. Bruno, P. Minutolo, and A. D'Anna, Proceedings of the Combustion Institute.
[8] A. D'Anna, M. Commodo, M. Sirignano, P. Minutolo, and R. Pagliara, Proceedings of the Combustion Institute **32 (**2009) 793-801.
[9] G. De Falco, M. Commodo, C. Bonavolontà, G.P. Pepe, P. Minutolo, and A. D'Anna, Combustion and Flame.
[10] A. Faccinetto, P. Desgroux, M. Ziskind, E. Therssen, and C. Focsa, Combustion and Flame **158 (**2011) 227-239.
[11] L.A. Sgro, A. D'Anna, and P. Minutolo, Combustion and Flame **158 (**2011) 1418-1425.
[12] M. Sirignano, M. Alfè, A. Tregrossi, A. Ciajolo, and A. D'Anna, Proceedings of the Combustion Institute **33 (**2011) 633-640.
[13] M. Sirignano, A. Collina, M. Commodo, P. Minutolo, and A. D'Anna, Combustion and Flame **159 (**2012) 1663-1669.
[14] M. Sirignano and A. D'Anna, Proceedings of the Combustion Institute **34 (**2013) 1877-1884.
[15] B. Hu, B. Yang, and U.O. Koylu, Combustion and Flame **134 (**2003) 93-106.
[16] J.H. Kent and D. Honnery, Combustion Science and Technology **54 (**1987) 383-398.
[17] B. Yang and U.O. Koylu, Combustion and Flame **141 (**2005) 55-65.
[18] N.H. Qamar, Z.T. Alwahabi, Q.N. Chan, G.J. Nathan, D. Roekaerts, and K.D. King, Combustion and Flame **156 (**2009) 1339-1347.
[19] M.E. Mueller, Q.N. Chan, N.H. Qamar, B.B. Dally, H. Pitsch, Z.T. Alwahabi, and G.J. Nathan, Combustion and Flame **160 (**2013) 1298-1309.
[20] V. Narayanaswamy and N.T. Clemens, Proceedings of the Combustion Institute **34 (**2013) 1455-1463.
[21] M. Köhler, K.-P. Geigle, T. Blacha, P. Gerlinger, and W. Meier, Combustion and Flame **159 (**2012) 2620-2635.
[22] A. Kronenburg, R.W. Bilger, and J.H. Kent, Combustion and Flame **121 (**2000) 24-40.
[23] M.E. Mueller and H. Pitsch, Combustion and Flame **159 (**2012) 2166-2180.
[24] M.E. Mueller and V. Raman, Combustion and Flame **161 (**2014) 1842-1848.
[25] H. El-Asrag, T. Lu, C.K. Law, and S. Menon, Combustion and Flame **150 (**2007) 108-126.
[26] H. El-Asrag and S. Menon, Combustion and Flame **156 (**2009) 385-395.
[27] P. Donde, V. Raman, M.E. Mueller, and H. Pitsch, Proceedings of the Combustion Institute **34 (**2013) 1183-1192.
[28] I.B. Berlman, *Handbook of Fluorescence Spectra of Aromatic Molecules*. 2 ed. 1971: Academic Press.
[29] T.M. F. Ossler, M. Ald, Cell Measurements **478 (**2001) 465-478.